Performance Comparison of MIMO Techniques for Optical Wireless Communications in Indoor Environments

Thilo Fath and Harald Haas, *Member, IEEE*

***Abstract*—In this paper, we compare the performance of multiple-input-multiple-output (MIMO) techniques applied to indoor optical wireless communications (OWC) assuming line-of-sight (LOS) channel conditions. Specifically, several 4×4 setups with different transmitter spacings and different positions of the receiver array are considered. The following MIMO algorithms are considered: Repetition Coding (RC), Spatial Multiplexing (SMP) and Spatial Modulation (SM). Particularly, we develop a framework to analytically approximate the bit error ratios (BERs) of these schemes and verify the theoretical bounds by simulations. The results show that due to diversity gains, RC is robust to various transmitter-receiver alignments. However, as RC does not provide spatial multiplexing gains, it requires large signal constellation sizes to enable high spectral efficiencies. In contrast, SMP enables high data rates by exploiting multiplexing gains. In order to provide these gains, SMP needs sufficiently low channel correlation. SM is a combined MIMO and digital modulation technique. We show that SM is more robust to high channel correlation compared to SMP, while enabling larger spectral efficiency compared to RC. Moreover, we investigate the effect of induced power imbalance between the multiple transmitters. It is found that power imbalance can substantially improve the performance of both SMP and SM as it reduces channel correlation. In this context, we also show that blocking some of the links is an acceptable method to reduce channel correlation. Even though the blocking diminishes the received energy, it outweighs this degradation by providing improved channel conditions for SMP and SM. For example, blocking 4 of the 16 links of the 4×4 setup improves the BER performance of SMP by more than 20 dB, while the effective signal to noise ratio (SNR) is reduced by about 2 dB due to the blocking. Therefore, MIMO techniques can provide gains even under LOS conditions which provide only little channel differences.**

***Index Terms*—MIMO, optical wireless communications, repetition coding, spatial modulation, spatial multiplexing.**

I. Introduction

RECENTLY, there has been increasing interest in OWC because of the tremendous advancements in solid-state-lighting technology. It is now possible to harnesses vast, free and largely unused wireless transmission resources in the infra-red (IR) and visible light spectrum for communication purposes. Especially for indoor scenarios, like office and home environments, OWC can provide significant spectrum relief for the crowed radio frequency (RF) spectrum used by traditional wireless communications systems such as wireless local area networks (WLANs). As more and more wireless home networks are being installed, the public ISM (Industrial, Scientific and Medical) band gets increasingly crowded leading to a shortage of available bandwidth, increased interference and compromised system throughput. In addition, RF communications can interfere with electrical equipment preventing its application in sensitive environments like hospitals or aircraft cabins.

With the advent of high luminance light-emitting diodes (LEDs), efficient and inexpensive illumination devices are available which will progressively replace existing light bulbs and fluorescent lamps. In contrast to the latter, LEDs, being electronic devices, can be switched must faster. Therefore, an additional benefit can be generated if LEDs are not only used for illumination, but also for high data rate wireless communications to establish flexible and ubiquitous communication networks [1]-[3]. For instance, the ceiling lights in an office can be used to transmit data to a receiver placed on a desk within a room. Apart from the visible light spectrum, the near-IR band between about 780 nm and 950 nm is also a potential transmission medium for indoor communications [4], [5]. Commonly, OWC transfers data by modulating the intensity of the optical signal [6]. Typical light fixtures achieve more than 400 lux to provide sufficient indoor illumination. Those illumination levels are enough to transmit data at high SNRs. At the receiver side, a photo-detector converts the optical signals into electrical signals which are used to decode the information. This direct detection enables the implementation of simple low-cost transceiver devices without the need for complex high-frequency circuit designs. As the information can only be received by a photo-detector which is within the emitted light beam and the signals do not penetrate opaque boundaries, the propagation can be restricted to specific spots or areas (rooms). This prevents interception and creates less interference compared to RF devices whose signals propagate through walls. Moreover, the LOS characteristic between transmitter and receiver can provide high SNRs of more than 60 dB at the receiver [7], [8].

In order to provide sufficient illumination, light installations are typically equipped with multiple LEDs. This property can readily be exploited to create optical MIMO communication systems. MIMO techniques are well-established and widely implemented in many RF systems as they offer high data

Paper approved by J. A. Salehi, the Editor for Optical CDMA of the IEEE Communications Society. Manuscript received August 29, 2011; revised May 15 and August 13, 2012.

This work was presented in part at the IEEE Global Communications Conference (GLOBECOM 2011), Houston, Texas, USA.

T. Fath is with EADS Deutschland GmbH, Innovation Works, 81663 Munich, Germany and with the University of Edinburgh, Institute for Digital Communications, the Kings Buildings, Edinburgh EH9 3JL, UK (e-mail: thilo.fath@ed.ac.uk).

H. Haas is with the University of Edinburgh, Institute for Digital Communications, the Kings Buildings, Edinburgh EH9 3JL, UK (e-mail: h.haas@ed.ac.uk).

Digital Object Identifier 10.1109/TCOMM.2012.120512.110578

rates by increasing the spectral efficiency [9], [10]. Off-the-shelf LEDs provide only a limited bandwidth of about $30-50$ MHz for incoherent IR light and even less for visible light. Consequently, these incoherent light sources restrict the available bandwidth of practical OWC systems. Therefore, it is equally important to achieve high spectral efficiencies in OWC. For free-space optical transmission the effects of MIMO have already been studied. It has been shown that spatial diversity can combat the fading effects due to scattering and scintillation caused by atmospheric turbulences [11], [12]. Ongoing research activities intend to increase the capacity of OWC indoor systems by MIMO techniques [13], [14]. However, for indoor OWC it is still not clear to what extent MIMO techniques can provide gains. This is because in indoor environments there are no fading effects caused by turbulence etc., especially if LOS scenarios are considered. Therefore, indoor optical wireless links are envisaged to be highly correlated enabling only minor diversity gains. Provided that MIMO techniques mostly rely on spatially uncorrelated channels, it is unclear whether the optical propagation channel in indoor environments can offer sufficiently low channel correlation.

In this paper, we study the performance of MIMO techniques for OWC in an indoor environment with LOS characteristic. A simple 4×4 setup with different transmitter spacings is assumed. We consider three different transmission schemes, namely RC, SMP and SM. These techniques are compared with regard to their BER performance for different spectral efficiencies. The error ratios are determined by computer simulations as well as by analytical approximations. For the latter, we give a framework to determine the theoretical BERs of the considered techniques using union bound methods. Moreover, we study the effect of induced power imbalance between the multiple transmitters. It has been shown in [15] that for a two-transmitter OWC scenario with highly correlated channels, power imbalance can improve the performance of MIMO. In addition, we investigate link blockage as a means to reduce channel correlation.

The remainder of this paper is organised as follows: In Section II we define the basic system model and the considered indoor system setup. The different MIMO techniques are introduced in Section III and their theoretical bit error bounds are determined. In Section IV we analyse the BER performance of the MIMO techniques for different scenarios. In this context, we investigate the effect of both induced power imbalance and link blockage. Finally, Section V concludes the paper.

II. System Model

We consider an optical wireless MIMO transmission system employing intensity modulation (IM) and direct detection (DD) of the optical carrier using incoherent light sources, *e.g.* LEDs. The system is equipped with N_t transmitters and N_r photo-detectors at the receiver side. The received signal vector is

$$\mathbf{y} = \mathbf{H}\,\mathbf{s} + \mathbf{n}, \tag{1}$$

where $\mathbf{n}$ is the sum of ambient shot light noise and thermal noise. It is independent of the transmitted signals and the main noise impairment as commonly assumed in OWC [5].

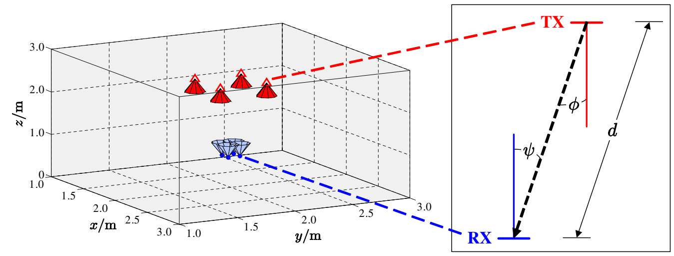

Fig. 1. Geometric scenario used for calculation of channel coefficients.

Consequently, $\mathbf{n}$ is real valued additive white Gaussian noise (AWGN) with zero mean and a variance $\sigma^2 = \sigma^2_{\text{shot}} + \sigma^2_{\text{thermal}}$, where σ^2_{shot} is the shot noise variance and $\sigma^2_{\text{thermal}}$ is the thermal noise variance [5]. Thus, the noise power is given by $\sigma^2 = N_0\,B$, where N_0 is the noise power spectral density and B is the bandwidth. The transmitted signal vector is denoted by $\mathbf{s} = [s_1\ \ldots\ s_{N_t}]^T$, with $[\cdot]^T$ being the transpose operator. The elements of $\mathbf{s}$ indicate which signal is emitted by each optical transmitter, *i.e.* s_{n_t} denotes the signal emitted by transmitter n_t. The $N_r \times N_t$ channel matrix $\mathbf{H}$ is given by

$$\mathbf{H} = \begin{pmatrix} h_{11} & \cdots & h_{1N_t} \\ \vdots & \ddots & \vdots \\ h_{N_r1} & \cdots & h_{N_rN_t} \end{pmatrix}, \tag{2}$$

where $h_{n_rn_t}$ represents the transfer factor of the wireless link between transmitter n_t and receiver n_r. As the LEDs are in close proximity, they can be jointly driven by exactly the same baseband hardware and electronic driver. We, therefore, assume that the transmission is perfectly synchronised. In addition, there is only a very small path difference between the multiple transmitter-receiver links of some cm (as shown in Section IV). Therefore, there is negligible temporal delay between the multiple links and consequently, we consider the system model given in (1) without time dispersion.

In this paper, we assume optical wireless links with LOS characteristics. Fig. 1 (right hand side) illustrates a directed LOS link. As shown, ϕ is the angle of emergence with respect to the transmitter (TX) axis and ψ is the angle of incidence with respect to the receiver (RX) axis. Furthermore, d depicts the distance between transmitter and receiver. Using this geometric scenario, the channel gain of an optical propagation link can be calculated according to [5] as follows:

$$h = \begin{cases} \frac{(k+1)\,A}{2\,\pi\,d^2}\cos^k(\phi)\cos(\psi) & 0 \le \psi \le \Psi_{\frac{1}{2}} \\ 0 & \psi > \Psi_{\frac{1}{2}} \end{cases} \tag{3}$$

with the order $k = \frac{-\ln(2)}{\ln\left(\cos(\Phi_{\frac{1}{2}})\right)}$ and the transmitter semiangle $\Phi_{\frac{1}{2}}$ (at half power), which is assumed to be $15°$. Furthermore, $\Psi_{\frac{1}{2}}$ denotes the field-of-view (FOV) semiangle of the receiver, which is assumed to be $15°$. These semiangles have been chosen with regard to a practical LOS indoor OWC system which has been developed and implemented within the European Union (EU) project OMEGA [16], [17]. A is the detector area of the receiver. In this paper, we assume A to be 1 cm^2. Clearly, the channel coefficient $h_{n_rn_t}$ depends on the specific position of transmitter n_t and receiver n_r. If a receiver and a transmitter are not in each others FOV, $h_{n_rn_t} = 0$.

$$\mathrm{BER}_{\mathrm{RC}} \geq \frac{2\,(M-1)}{M\,\log_2(M)}\,\mathrm{Q}\left(\frac{1}{M-1}\sqrt{\frac{E_s}{N_0\,N_t^2}\,\sum_{n_r=1}^{N_r}\left(\sum_{n_t=1}^{N_t} h_{n_r n_t}\right)^2}\right) \quad (7)$$

In the following, we consider a 4×4 indoor scenario ($N_r = 4$ and $N_t = 4$) which is located within a $4.0\,\mathrm{m} \times 4.0\,\mathrm{m} \times 3.0\,\mathrm{m}$ room. We assume that the transmitters are placed at a height of $z = 2.50$ m and are oriented downwards to point straight down from the ceiling. The receivers are located at a height of $z = 0.75$ m (*e.g.* height of a table) and are oriented upwards to point straight up at the ceiling. Both transmitters and receivers are aligned in a quadratically 2×2 array which is centered in the middle of the room. On the basis of this scenario, we investigate different static setups with varying spacings of the single transmitters on the x- and y-axis, depicted by d_{TX}. The spacing of the receivers is assumed to be 0.1 m on the x- and y-axis for all considered setups. This receiver spacing would enable the implementation of the receiver array into typical laptop computers. Fig. 1 (left hand side) shows the positioning of the 4×4 setup. The receivers are displayed as dots and the transmitters as triangles. The plotted cones represent the orientation of the transmit beams and the orientation of the FOVs of the receivers, respectively. The cone angles are related to the semiangles of the transmitter and receiver devices.

III. MIMO Techniques

In the following, we introduce the different MIMO techniques which we study for indoor OWC. We assume that all considered MIMO techniques use maximum-likelihood (ML) detection at the receiver side with perfect knowledge of the channel and ideal time synchronisation. Therefore, the decoder decides for the constellation vector $\widehat{\mathbf{s}}$ which minimises the Euclidean distance between the actual received signal vector $\mathbf{y}$ and all potential received signals leading to

$$\widehat{\mathbf{s}} = \arg\max_{\mathbf{s}} p_{\mathbf{y}}(\mathbf{y}|\mathbf{s},\mathbf{H}) = \arg\min_{\mathbf{s}} \|\mathbf{y} - \mathbf{H}\,\mathbf{s}\|_{\mathrm{F}}^2\,, \quad (4)$$

where $p_{\mathbf{y}}$ is the probability density function of $\mathbf{y}$ conditioned on $\mathbf{s}$ and $\mathbf{H}$. $\|\cdot\|_{\mathrm{F}}$ denotes the Frobenius norm.

The simplest MIMO transmission technique is RC which simultaneously emits the same signal from all transmitters. Therefore, for RC $s_1 = s_2 = \ldots = s_{N_t}$ holds. RC is known to achieve good performance in free-space OWC because of transmit-diversity [12]. In [18] it is shown that RC can outperform orthogonal space-time block codes (OSTBCs) like the Alamouti scheme [19] and single-input-multiple-output (SIMO) setups. This is due to the fact that the intensities coming from the several transmitters constructively add up at the receiver side. In this paper, unipolar M-level pulse amplitude modulation (M-PAM) is considered together with RC, where M denotes the signal constellation size. Consequently, M-PAM achieves a spectral efficiency of $\log_2(M)$ bit/s/Hz. We consider PAM because it is more bandwidth efficient compared to other pulse modulation techniques such as on-off-keying (OOK), pulse width modulation (PWM) and pulse position modulation (PPM). Moreover, PAM has shown to have similar optical power efficiency compared to direct-current-biased optical orthogonal frequency division multiplexing (DCO-OFDM) [20]. For instance, in [21] and [22] the authors show that PAM outperforms DCO-OFDM because the latter requires a high constant DC bias to make the bipolar OFDM waveform non-negative. This DC bias power affects the effective SNR of DCO-OFDM in contrast to unipolar PAM which operates without an additional DC bias. Without loss of generality, we employ rectangular pulses in conjunction with M-PAM. The intensity levels are given by:

$$I_m^{\mathrm{PAM}} = \tfrac{2\,I}{M-1}\,m \quad \text{for } m = 0, 1, \ldots, (M-1), \quad (5)$$

where I is the mean optical power emitted. According to, for instance, [6], the BER of unipolar M-PAM can be lower bounded by

$$\mathrm{BER}_{\mathrm{PAM}} \geq \frac{2\,(M-1)}{M\,\log_2(M)}\,\mathrm{Q}\left(\frac{1}{M-1}\sqrt{\frac{E_{\mathrm{RX}}}{N_0}}\right), \quad (6)$$

where $\mathrm{Q}(a) = \frac{1}{\sqrt{2\pi}}\int_a^{+\infty}\exp(\frac{-t^2}{2})\,\mathrm{d}t$ is the Q-function and E_{RX} is the *received* electrical energy. In the following, $E_s = (r\,I)^2\,T_s$ denotes the mean *emitted* electrical energy of the intensity modulated optical signals. r represents the optical-to-electrical conversion coefficient. Without loss of generality, we assume r to be 1 A$\sqrt{\Omega}$/W. T_s denotes the symbol duration in seconds. As RC simultaneously emits the same signal from several transmitters, the optical transmission power is equally distributed across all emitters. Thus, the intensities given in (5) have to be divided by factor N_t. By doing so, the mean optical power emitted is constant, irrespective of the number of employed transmitters. This ensures the comparability of different setups and transmission techniques. The BER of M-PAM given in (6) can be generalised for an arbitrary $N_r \times N_t$ scenario which employs RC. The BER of RC is shown in (7) on top of this page. The intensities emitted by the multiple transmitters constructively add up at the receiver leading to an optical power of $I_{\mathrm{RX}_{n_r}} = \sum_{n_t=1}^{N_t} \frac{I}{N_t}\,h_{n_r n_t}$ at receiver n_r. Consequently, the single channel gains $h_{n_r n_t} \in [0;1]$ induce a distinctive attenuation of the transmitted signals (path loss) depending on the specific link characteristic. The N_r received signals are combined by maximum ratio combining (MRC) [23, Ch. 7.2.4]. Thus by applying MRC, the received signals with a high SNR are weighted more than signals with a low SNR. Consequently, the electrical SNR after the combiner becomes:

$$\begin{aligned} \frac{E_{\mathrm{RX}}}{N_0} &= \frac{T_s}{N_0}\sum_{n_r=1}^{N_r}\left(r\,I_{\mathrm{RX}_{n_r}}\right)^2 \\ &= \frac{T_s}{N_0}\sum_{n_r=1}^{N_r}\left(\sum_{n_t=1}^{N_t}\frac{r\,I}{N_t}\,h_{n_r n_t}\right)^2 \\ &= \frac{E_s}{N_0\,N_t^2}\sum_{n_r=1}^{N_r}\left(\sum_{n_t=1}^{N_t} h_{n_r n_t}\right)^2, \end{aligned} \quad (8)$$

$$\mathrm{BER}_{\mathrm{SMP}} \leq \frac{1}{M^{N_t}\,\log_2(M^{N_t})} \sum_{m^{(1)}=1}^{M^{N_t}} \sum_{m^{(2)}=1}^{M^{N_t}} \mathrm{d}_{\mathrm{H}}(b_{m^{(1)}}, b_{m^{(2)}})\,\mathrm{Q}\left(\sqrt{\frac{r^2\,T_s}{4\,N_0}\,\left\|\mathbf{H}\left(\mathbf{s}_{m^{(1)}} - \mathbf{s}_{m^{(2)}}\right)\right\|_{\mathrm{F}}^2}\right) \tag{10}$$

which corresponds to the SNR given in the argument of the Q-function in (7). Moreover, (8) comprises the received electrical energy given by $E_{\mathrm{RX}} = \sum_{n_r=1}^{N_r} \left(r\,I_{\mathrm{RX}_{n_r}}\right)^2 T_s$. Consequently, the given BER of RC is only affected by the transfer factors of the wireless optical links, respectively by the received optical power. Thus, RC can be represented by a simple single-input-single-output (SISO) scheme which provides the same received electrical energy.

Another well-known MIMO technique is SMP. By applying SMP, independent data streams are simultaneously emitted from all transmitters. Therefore, SMP provides an enhanced spectral efficiency of $N_t\,\log_2(M)$ bit/s/Hz. Like for RC, we use PAM for SMP and equally distribute the optical power across all emitters to ensure that both schemes use the same mean transmission power. For SMP, the signal vector $\mathbf{s}$ has N_t elements which are independent M-PAM modulated signals according to (5), whereas their respective emitted intensities are divided by N_t. Provided that the SMP receiver performs a ML detection, the pairwise error probability (PEP) is the probability that the receiver mistakes the transmitted signal vector $\mathbf{s}_{m^{(1)}}$ for another vector $\mathbf{s}_{m^{(2)}}$, given knowledge of the channel matrix $\mathbf{H}$. Thus, the PEP of SMP can be calculated by

$$\begin{aligned}\mathrm{PEP}_{\mathrm{SMP}} &= \mathrm{PEP}(\mathbf{s}_{m^{(1)}} \rightarrow \mathbf{s}_{m^{(2)}}|\mathbf{H}) \\ &= \mathrm{Q}\left(\sqrt{\frac{r^2\,T_s}{4\,N_0}\,\left\|\mathbf{H}\left(\mathbf{s}_{m^{(1)}} - \mathbf{s}_{m^{(2)}}\right)\right\|_{\mathrm{F}}^2}\right).\end{aligned} \tag{9}$$

Using this PEP and considering all M^{N_t} possible combinations of the transmitted signal vector, the BER of SMP can be approximated by union bound methods. The upper bound is given in (10) on top of this page, with $\mathrm{d}_{\mathrm{H}}(b_{m^{(1)}}, b_{m^{(2)}})$ denoting the Hamming distance of the two bit assignments $b_{m^{(1)}}$ and $b_{m^{(2)}}$ of the signal vectors $\mathbf{s}_{m^{(1)}}$ and $\mathbf{s}_{m^{(2)}}$. For instance, if we assume $N_t = 4$ and $M = 2$, the bit sequence "$1\,0\,0\,1$" is assigned to $\mathbf{s}_{10} = \left[\frac{I}{2}\ 0\ 0\ \frac{I}{2}\right]^T$ and "$1\,0\,0\,0$" is assigned to $\mathbf{s}_9 = \left[\frac{I}{2}\ 0\ 0\ 0\right]^T$, resulting in $\mathrm{d}_{\mathrm{H}}(b_{10}, b_9) = 1$. Therefore, $\mathrm{d}_{\mathrm{H}}(\cdot,\cdot)$ states the number of bit errors when erroneously detecting $\mathbf{s}_{m^{(2)}}$ at the receiver instead of the actually transmitted signal vector $\mathbf{s}_{m^{(1)}}$.

Finally, we also consider SM, which is a combined MIMO and digital modulation technique, proposed in [24] and further investigated in [25]-[27]. In SM, the conventional signal constellation diagram is extended to an additional dimension, namely the spatial dimension. The spatial dimension is used to transmit additional bits. Each transmitter in the transmitting array is assigned a unique binary sequence – the spatial symbol. A transmitter is only activated when the random spatial symbol to be transmitted matches the pre-allocated spatial symbol. Thus, only one transmitter is activated at any PAM symbol duration. Therefore, only one element of the signal vector $\mathbf{s}$ to be transmitted is non-zero. The element is

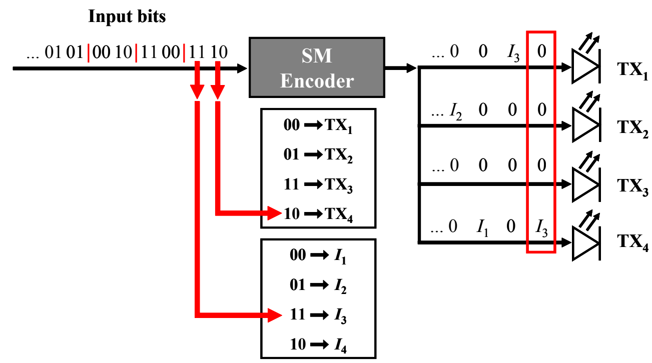

Fig. 2. Illustration of SM operation with $N_t = 4$ and $M = 4$. The first two bits in the block of four bits determine the PAM symbol and the second two bits determine the active LED.

the digitally modulated signal to be sent. The index of the non-zero element is the spatial symbol. SM simultaneously transmits data in the signal domain and the spatial domain. Consequently, SM provides an enhanced spectral efficiency of $\log_2(N_t) + \log_2(M)$ bit/s/Hz. Moreover, as only one transmitter is activated at any symbol duration, SM completely avoids inter-channel interference (ICI). Thus, SM has a lower decoding complexity compared to other MIMO schemes [28]-[30]. Due to the distinct channel transfer factors between a particular transmitter and the receiver, the receiver is able to detect which transmitter is activated and hence is able to detect the spatial symbol. Fig. 2 illustrates the functionality of SM for a setup with $N_t = 4$ optical emitters and a signal constellation size of $M = 4$. The bits to be transmitted are passed to the SM encoder, which maps them to the respective signal and transmitter index. In this example, the last two bits denote the index of the transmitter which emits the signal, whereas the first two bits represent the actual signal to be sent. For instance, the bit sequence "$1\,1\,1\,0$" is represented by transmitter number 4 emitting signal I_3. In contrast to RC and SMP, signals with intensity $I_m = 0$ cannot be used for the signal modulation of SM. Because in this case, no transmitter would be active and the spatial information would be lost. Therefore, the intensities of common PAM given in (5) have to be modified to be suitable for SM leading to:

$$I_m^{\mathrm{SM}} = \tfrac{2\,I}{M+1}\,m \quad \text{for } m = 1\ldots M. \tag{11}$$

Consequently, the minimum distance between two SM signals is $\frac{2\,I}{M+1}$, whereas the minimum distance for common PAM is $\frac{2\,I}{M-1}$. The smaller signal distance of SM might induce a worse BER performance because the error probability depends on the Euclidean distance of the transmitted signals. However, as SM additionally encodes data bits in the spatial domain, it can provide the same spectral efficiency as common M-PAM with a lower signal constellation size, hence effectively enlarging the distance of the signal points. As the SM receiver has to detect which transmitter has sent the signal, its performance depends on the differentiability of the multiple channels. Thus,

$$\begin{aligned}\mathrm{BER}_{\mathrm{SM}} \leq \frac{1}{MN_t\ \log_2(MN_t)} \sum_{m^{(1)}=1}^{M} \sum_{n_t^{(1)}=1}^{N_t} \sum_{m^{(2)}=1}^{M} \sum_{n_t^{(2)}=1}^{N_t} \mathrm{d_H}\left(b_{m^{(1)} n_t^{(1)}}, b_{m^{(2)} n_t^{(2)}}\right) \cdot \\ \mathrm{Q}\left(\sqrt{\frac{r^2\,T_s}{4\,N_0} \sum_{n_r=1}^{N_r} \left| I_{m^{(2)}}^{\mathrm{SM}}\ h_{n_r n_t^{(2)}} - I_{m^{(1)}}^{\mathrm{SM}}\ h_{n_r n_t^{(1)}} \right|^2}\right)\end{aligned} \tag{13}$$

the performance of SM is affected by the channel correlation. The PEP of SM is

$$\begin{aligned}\mathrm{PEP}_{\mathrm{SM}} &= \mathrm{PEP}(\mathbf{s}_{m^{(1)}} \to \mathbf{s}_{m^{(2)}}|\mathbf{H}) \\ &= \mathrm{Q}\left(\sqrt{\frac{r^2\,T_s}{4\,N_0}\ \left\|\mathbf{H}\left(\mathbf{s}_{m^{(1)}} - \mathbf{s}_{m^{(2)}}\right)\right\|_{\mathrm{F}}^2}\right) \\ &= \mathrm{Q}\left(\sqrt{\frac{r^2\,T_s}{4\,N_0} \sum_{n_r=1}^{N_r} \left| I_{m^{(2)}}^{\mathrm{SM}}\ h_{n_r n_t^{(2)}} - I_{m^{(1)}}^{\mathrm{SM}}\ h_{n_r n_t^{(1)}} \right|^2}\right).\end{aligned} \tag{12}$$

This denotes the probability that the receiver decides for intensity $I_{m^{(2)}}^{\mathrm{SM}}$ being emitted by transmitter $n_t^{(2)}$, whereas actually transmitter $n_t^{(1)}$ has emitted intensity $I_{m^{(1)}}^{\mathrm{SM}}$. Using this PEP and considering all possible MN_t signal combinations, the BER of SM can be approximated by union bound methods. The upper bound of its BER is given in (13) on top of this page, where $b_{m^{(1)} n_t^{(1)}}$ is the bit assignment which is conveyed when intensity $I_{m^{(1)}}^{\mathrm{SM}}$ is emitted by transmitter $n_t^{(1)}$ and $b_{m^{(2)} n_t^{(2)}}$ is the bit assignment which is encoded when intensity $I_{m^{(2)}}^{\mathrm{SM}}$ is emitted by transmitter $n_t^{(2)}$. Consequently, $\mathrm{d_H}\left(b_{m^{(1)} n_t^{(1)}}, b_{m^{(2)} n_t^{(2)}}\right)$ states the number of bit errors when erroneously decoding the bit sequence $b_{m^{(2)} n_t^{(2)}}$ at the receiver instead of the actually transmitted sequence $b_{m^{(1)} n_t^{(1)}}$.

IV. Results on Bit Error Ratio Performance

In this section, we analyse the BER performance of the MIMO techniques introduced in Section III by considering several setup scenarios which are based on the model presented in Section II. In order to ensure comparability, the mean emitted optical power is the same for each scenario as well as for all MIMO techniques. We evaluate the error ratios at the receiver side with regard to *transmit* energy against power spectral density of the AWGN. Hence, we take into account the specific path loss of each setup caused by the particular distance and angular alignment of the single transmitters and receivers. Consequently, we define the SNR as $\frac{E_s}{N_0}$. This is because considering received energy to noise energy would disregard the individual path loss of the different setups, thus disallowing a fair performance comparison.

We consider the 4×4 setup with transmitter spacings on the x- and y-axis of $d_{\mathrm{TX}} = 0.2, 0.4$ and 0.6 m. Applying (3) to these scenarios gives the following channel matrices (without noise):

$$\begin{aligned}\mathbf{H}_{d_{\mathrm{TX}}=0.2} &\approx\ 10^{-4} \begin{pmatrix} 1.0708 & 0.9937 & 0.9937 & 0.9226 \\ 0.9937 & 1.0708 & 0.9226 & 0.9937 \\ 0.9937 & 0.9226 & 1.0708 & 0.9937 \\ 0.9226 & 0.9937 & 0.9937 & 1.0708 \end{pmatrix}, \\ \mathbf{H}_{d_{\mathrm{TX}}=0.4} &\approx\ 10^{-4} \begin{pmatrix} 0.9226 & 0.7964 & 0.7964 & 0.6888 \\ 0.7964 & 0.9226 & 0.6888 & 0.7964 \\ 0.7964 & 0.6888 & 0.9226 & 0.7964 \\ 0.6888 & 0.7964 & 0.7964 & 0.9226 \end{pmatrix}, \\ \mathbf{H}_{d_{\mathrm{TX}}=0.6} &\approx\ 10^{-4} \begin{pmatrix} 0.6888 & 0.5559 & 0.5559 & 0.0000 \\ 0.5559 & 0.6888 & 0.0000 & 0.5559 \\ 0.5559 & 0.0000 & 0.6888 & 0.5559 \\ 0.0000 & 0.5559 & 0.5559 & 0.6888 \end{pmatrix}.\end{aligned} \tag{14}$$

The symmetrical arrangement of the transmitters and receivers leads to equal channel gains for the links with the same geometrical alignment. Moreover, if the spacing between the transmitters is small, the gains are quite similar, whereas if d_{TX} gets larger, the differences between the links increase. If $d_{\mathrm{TX}} = 0.6$ m, some transmitters and receivers are not in each others FOV resulting in $h_{n_r n_t} = 0$. As the channel coefficients are in the region of 10^{-4}, the electrical path loss at the receiver side is about -80 dB. Because we defined the SNR as the ratio of *transmitted* signal energy to noise, the BER curves displayed in the following figures have an SNR offset of about 80 dB with respect to the *received* energy to noise ratio. Furthermore, if we consider the diffuse transmission portion induced by first order reflections on the surfaces (walls), the reflected optical intensity impinging on the receivers is in the range of $10^{-10}\,I$ (assuming ideal conditions such as Lambertian reflectors and a reflectivity of $\rho = 1$). This results in an electrical path loss which is about $110 - 120$ dB larger than the path loss of the LOS transmission. As the path loss of higher order reflections is even larger, we can neglect reflections in the following and consider only the LOS gains given in (14) without any diffuse transmission portions. However, additional multipath reflections would enhance the differentiability of the MIMO channels and would reduce the channel correlation. Hence, as there are no reflections, the considered LOS scenario is subject to highly correlated links and constitutes a worst case scenario with regard to channel correlation.

Enlarging d_{TX} increases the path loss. Therefore, the impairment in received energy can be denoted for different transmitter spacings:

$$\Delta_{d_{\mathrm{TX}}=x}^{E_{\mathrm{RX}}} = 10\ \log_{10}\left(\frac{E_{\mathrm{RX}_{d_{\mathrm{TX}}=x}}}{E_{\mathrm{RX}_{d_{\mathrm{TX}}=0.2}}}\right). \tag{15}$$

$E_{\mathrm{RX}_{d_{\mathrm{TX}}=x}}$ denotes the received electrical energy for $d_{\mathrm{TX}} = x$ m. The impairment is related to the $d_{\mathrm{TX}} = 0.2$ m setup which provides the lowest path loss yielding to

$$\begin{aligned} \Delta^{E_{\mathrm{RX}}}_{d_{\mathrm{TX}}=0.2} &= \quad 0.00\,\mathrm{dB}, \\ \Delta^{E_{\mathrm{RX}}}_{d_{\mathrm{TX}}=0.4} &\approx -1.88\,\mathrm{dB}, \\ \Delta^{E_{\mathrm{RX}}}_{d_{\mathrm{TX}}=0.6} &\approx -6.89\,\mathrm{dB}. \end{aligned} \tag{16}$$

Besides, the maximum difference in path length of the multiple transmitter-receiver links is about 33.30 mm. This difference results in a maximum delay variation of 111.06 ps. A delay variation of several ps only has an effect for switching speeds in the region of several GHz. As we consider off-the-shelf LEDs which provide a bandwidth of about $30 - 50$ MHz, we can neglect this delay variation and assume ideal synchronisation of all links without time dispersion.

Fig. 3(a) shows the BER performance of RC, SMP and SM for the three setup scenarios for a spectral efficiency of $R = 4$ bit/s/Hz. For $d_{\mathrm{TX}} = 0.2$ m and 0.4 m, RC gives the best performance, whereas SMP performs worst with a low slope of the BER curve within the depicted SNR range. This is due to the fact, that for both scenarios the channel gains are quite similar providing high channel correlation. Although the performance of SM also depends on the differences between the links, SM is more robust to these channel conditions. SM provides a lower error ratio and a steeper slope of the BER curve compared to SMP. If $d_{\mathrm{TX}} = 0.6$ m, SMP and SM outperform RC at a BER of 10^{-5} by about 10 dB, respectively by 9 dB. RC performs about 7 dB worse compared to the $d_{\mathrm{TX}} = 0.2\,\mathrm{m}$ case because of less received energy as $\Delta^{E_{\mathrm{RX}}}_{d_{\mathrm{TX}}=0.6} \approx -6.89$ dB. Despite this larger path loss for $d_{\mathrm{TX}} = 0.6$ m, SMP and SM even outperform RC for the two other scenarios, which provide a lower path loss. SMP outperforms SM by about 1 dB for high SNRs. Because of its multiplexing gain, SMP can operate with a reduced signal constellation size of $M = 2$ as opposed to SM which has to operate with $M = 4$ to provide the same data rate. But at low SNR regions of up to about 103 dB, SM provides the best BER performance. This implies that SM profits from conveying information in the spatial domain especially at low SNRs. Whereas at high SNR regions SM suffers from the fact that it has to use a larger signal constellation size to provide the same spectral efficiency as SMP. Accordingly, SMP requires a high SNR to separate the single signal streams at the receiver side and to benefit from its multiplexing gain. Moreover, the theoretical lower and upper error bounds (shown by markers) given in (7), (10) and (13) closely match the simulation results (shown by lines). Thus, the error bounds provide an accurate approximation of the BERs at high SNRs.

Fig. 3(b) shows the BER performance of the three schemes for the same setup scenarios but with an enhanced spectral efficiency of $R = 8$ bit/s/Hz. RC requires an SNR increase of about 24 dB to achieve the same BER of 10^{-5} compared to the $R = 4$ bit/s/Hz case. For $d_{\mathrm{TX}} = 0.2$ m and $d_{\mathrm{TX}} = 0.4$ m, SMP still performs worst. However, SM outperforms RC up to an SNR of about 130 dB for $d_{\mathrm{TX}} = 0.2$ m, respectively 134 dB for $d_{\mathrm{TX}} = 0.4$ m. If $d_{\mathrm{TX}} = 0.6$ m, SMP provides the best performance as it achieves an SNR benefit of about 25 dB compared to RC and of about 12 dB compared to SM. Hence, due to its multiplexing gain, SMP requires an SNR improvement of only 10 dB to provide the same BER performance when doubling the spectral efficiency from 4 to 8 bit/s/Hz, whereas SM needs additional 21 dB.

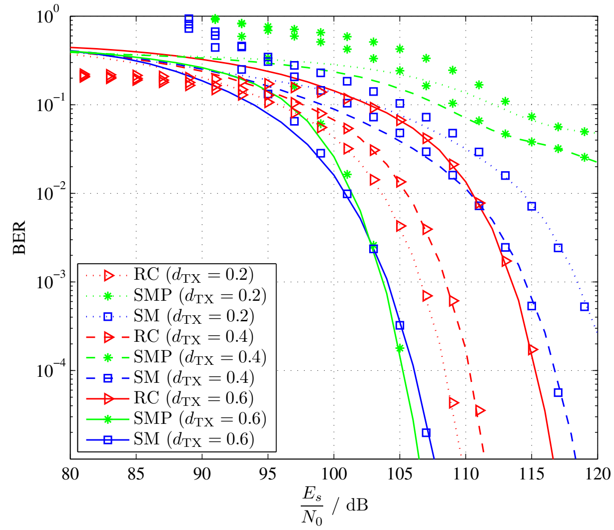

(a) $R = 4$ bit/s/Hz

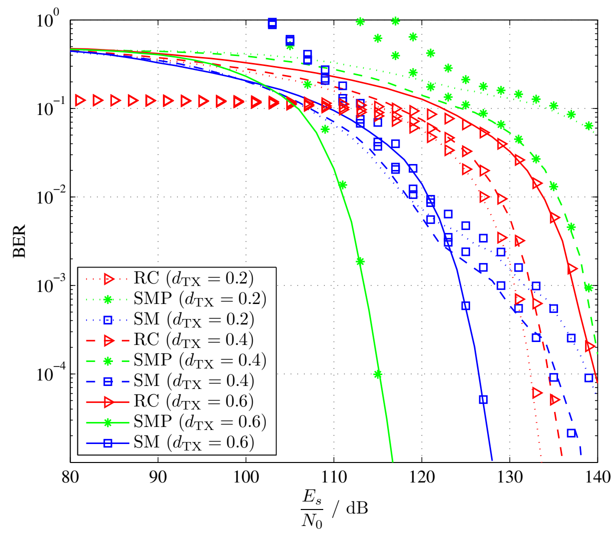

(b) $R = 8$ bit/s/Hz

Fig. 3. Comparison of RC, SMP and SM for spectral efficiency of $R = 4$ and $R = 8$ bit/s/Hz in 4×4 setup scenario with varying distance d_{TX} of transmitters on the x- and y-axis (lines show simulation results and markers analytical error bounds).

If we assume $d_{\mathrm{TX}} = 0.7\,\mathrm{m}$, we get

$$\mathbf{H}_{d_{\mathrm{TX}}=0.7} \approx 10^{-4} \begin{pmatrix} 0.5658 & 0 & 0 & 0 \\ 0 & 0.5658 & 0 & 0 \\ 0 & 0 & 0.5658 & 0 \\ 0 & 0 & 0 & 0.5658 \end{pmatrix}, \tag{17}$$

which results in an aligned system where only one transmitter and receiver are in each others FOV. This leads to a direct alignment with four completely independent links. Fig. 4 displays the BER results for a spectral efficiency of $R = 4$ and $R = 8$ bit/s/Hz for this scenario. In comparison to the $d_{\mathrm{TX}} = 0.6$ m scenario, all MIMO schemes perform

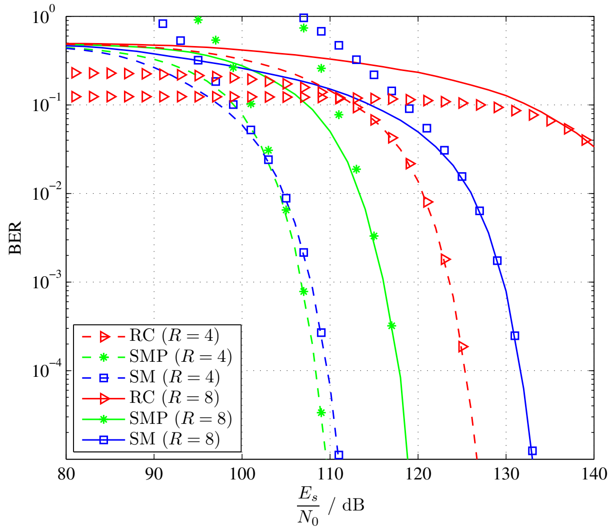

Fig. 4. Comparison of RC, SMP and SM for spectral efficiency of $R = 4$ and $R = 8$ bit/s/Hz in 4×4 setup scenario with $d_{\mathrm{TX}} = 0.7$ m (lines show simulation results and markers analytical error bounds).

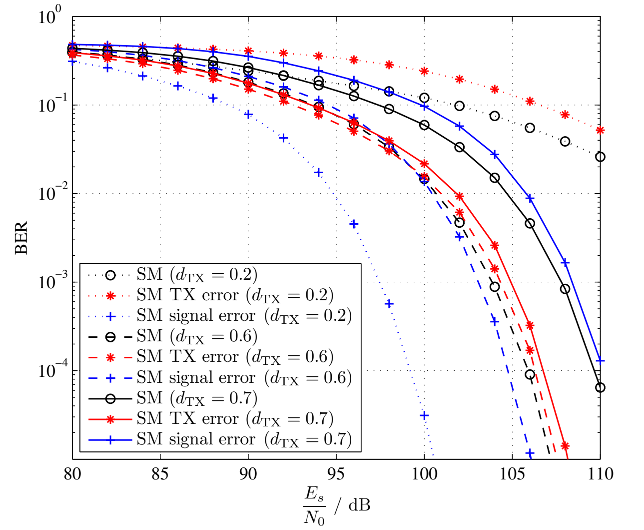

Fig. 5. BER of SM segmented into bit errors caused by transmitter misdetection and signal misdetection for spectral efficiency of $R = 4$ bit/s/Hz in 4×4 setup scenario with varying distance d_{TX} of transmitters on the x- and y-axis.

worse because there is less energy received. This is due to the missing cross-connects between emitter n_t and receiver n_r for $n_t \neq n_r$ leading to $\Delta^{E_{\mathrm{RX}}}_{d_{\mathrm{TX}}=0.7} \approx -16.95$ dB. Whereas SM and SMP undergo a minor performance decrease of only about 3 dB, the performance of RC is degraded by about 10 dB. Consequently, RC suffers much more from the direct alignment, whereas SMP and SM can compensate the less received energy by the reduced channel correlation. For $R = 4$ bit/s/Hz, SM again outperforms SMP at low SNR regions up to about 103 dB. At higher SNRs, SMP outperforms SM due to its larger multiplexing gain. This issue is even more evident for the $R = 8$ bit/s/Hz case, where SMP achieves major performance gains as it provides this spectral efficiency with $M = 4$ compared to SM which has to operate with $M = 64$.

In the following, we study why SM achieves performance gains especially in the low SNR region. Therefore, the BER of SM is segmented into errors arising from transmitter misdetection and from signal misdetection. If $R = 4$ bit/s/Hz, SM conveys the same number of bits in the spatial and in the signal domain. Fig. 5 shows that for $d_{\mathrm{TX}} = 0.2$ m, the errors caused by inaccurate detection of the transmitter mainly affect the BER, whereas the mere signal detection provides much lower error ratios. If $d_{\mathrm{TX}} = 0.6$ m, the transmitter detection provides a lower error ratio up to an SNR of about 99 dB, thus improving the overall BER of SM. At higher SNRs the signal detection can be performed more reliably and the errors caused by an erroneous detection of the transmitter get decisive again. In the aligned system ($d_{\mathrm{TX}} = 0.7$ m), the signal misdetection is the dominating source of errors due to less energy received. In contrast, the detection of the active emitter can be performed more reliably because the direct alignment provides the lowest channel correlation. Therefore, the inherent nature of SM, which is conveying information in the spatial domain, can be exploited most distinctively by direct alignment of the optical transmitters and receivers. Thus despite less energy received, independent links enable the most reliable detection of the active transmitter.

A. Varying position of receiver array

In this section, we consider the situation when the position of the receiver array is varied. We define x_{RX} and y_{RX} as the position offsets of the receiver array on the x- and y-axis relative to the center of the room. These offsets increase both the distance and the misalignment between the transmitter array and the receivers. In order to still be able to detect the TX beams, we assume a larger FOV semiangle of the receivers of $\Psi_{\frac{1}{2}} = 45°$. The considered position offsets are: i) $x_{\mathrm{RX}} = 0.5$ m, $y_{\mathrm{RX}} = 0$ m; ii) $x_{\mathrm{RX}} = 0.25$ m, $y_{\mathrm{RX}} = 0.75$ m and iii) $x_{\mathrm{RX}} = 0.5$ m, $y_{\mathrm{RX}} = 1.0$ m. Applying (3) to these scenarios results in the following channel matrices:

$$\mathbf{H}_{\mathrm{i}} \approx 10^{-4} \begin{pmatrix} 0.2293 & 0.2013 & 0.1462 & 0.1290 \\ 0.2013 & 0.2293 & 0.1290 & 0.1462 \\ 0.7964 & 0.6888 & 0.6410 & 0.5559 \\ 0.6888 & 0.7964 & 0.5559 & 0.6410 \end{pmatrix},$$
$$\mathbf{H}_{\mathrm{ii}} \approx 10^{-4} \begin{pmatrix} 0.0461 & 0.0272 & 0.0358 & 0.0213 \\ 0.2573 & 0.1798 & 0.1917 & 0.1352 \\ 0.0735 & 0.0424 & 0.0713 & 0.0412 \\ 0.4426 & 0.3040 & 0.4275 & 0.2940 \end{pmatrix}, \quad (18)$$
$$\mathbf{H}_{\mathrm{iii}} \approx 10^{-4} \begin{pmatrix} 0.0061 & 0.0035 & 0.0044 & 0.0025 \\ 0.0442 & 0.0283 & 0.0299 & 0.0194 \\ 0.0150 & 0.0082 & 0.0128 & 0.0071 \\ 0.1290 & 0.0792 & 0.1071 & 0.0663 \end{pmatrix}.$$

Fig. 6 shows the BER of RC, SMP and SM for a spectral efficiency of 8 bit/s/Hz in the 4×4 setup scenario with $d_{\mathrm{TX}} = 0.4$ m using these position offsets. The increased distance between the transmitters and the receivers leads to a larger path loss and an increased $\frac{E_s}{N_0}$ offset compared to the scenario with $x_{\mathrm{RX}} = y_{\mathrm{RX}} = 0$ m. However, the larger distance also increases the differences between the channels. This improves the performance of SMP. While SMP performs

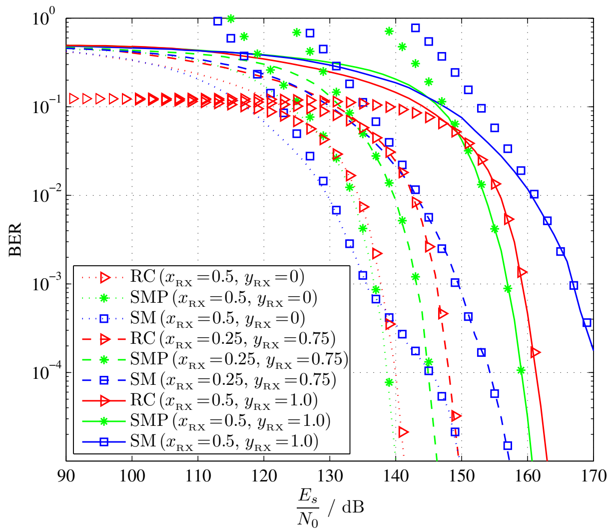

Fig. 6. Comparison of RC, SMP and SM for spectral efficiency of $R = 8$ bit/s/Hz in 4×4 setup scenario with $d_{\mathrm{TX}} = 0.4$ m and varying position offsets of receiver array on the x- and y-axis (lines show simulation results and markers analytical error bounds).

worst when the x-offset and y-offset are zero (due to channel similarities), it performs better than RC and SM when assuming position offsets and larger distances. This is because of favorable channel conditions and the fact that the spatial multiplexing gain of SMP grows linearly with the minimum number of transmitters and receivers. In contrast, the spatial multiplexing gain grows only logarithmically in the case of SM, and there is no spatial multiplexing gain in the case of RC.

B. Power imbalance between transmitters

In the following, we analyse the effect of induced power imbalance between the single transmitters. Thus, the transmission power is not uniformly distributed across all N_t transmitters but imbalanced. We define δ as the optical power imbalance factor in dB and $\alpha = 10^{\frac{\delta}{10}}$ as the imbalance factor on a linear scale. Therefore, α denotes the optical power surplus factor assigned to one transmitter in comparison to another one. Note that the mean optical power emitted by all transmitters, I, is still the same as before. This means that the total transmission power is not increased by driving individual LEDs in the array with different powers. Moreover, the power distribution is done without any channel state information at the transmitter.

The induced power imbalance factors for each transmitter can be calculated by

$$\gamma_1 = \frac{N_t}{\sum_{i=0}^{N_t-1} \alpha^i}, \qquad\qquad (19)$$
$$\gamma_{j+1} = \alpha\, \gamma_j \qquad \text{for } j = 1 \ldots N_t - 1.$$

For instance, if we assume $\delta = 3$ dB and $N_t = 4$, we get $\gamma_1 \approx \frac{4}{15}$, $\gamma_2 \approx \frac{8}{15}$, $\gamma_3 \approx \frac{16}{15}$ and $\gamma_4 \approx \frac{32}{15}$. Using these factors, the optical transmission power assigned to emitter n_t applying RC or SMP is $\tilde{I}_{n_t} = \frac{I}{N_t}\gamma_{n_t}$ and for SM it is $\tilde{I}_{n_t} = I\,\gamma_{n_t}$. Note that the signal modulation technique is still PAM according to

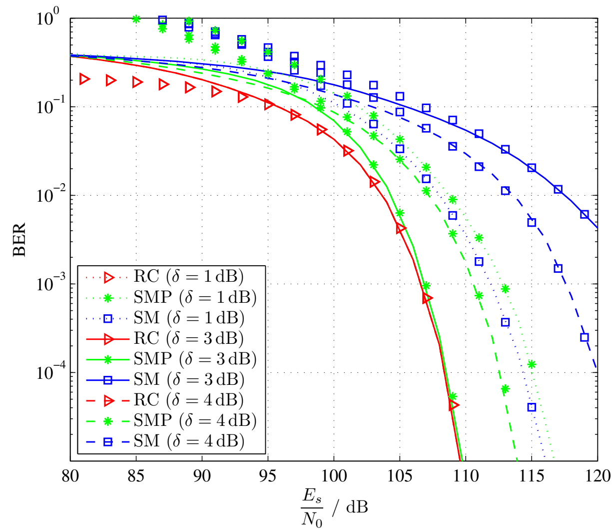

(a) $d_{\mathrm{TX}} = 0.2$ m

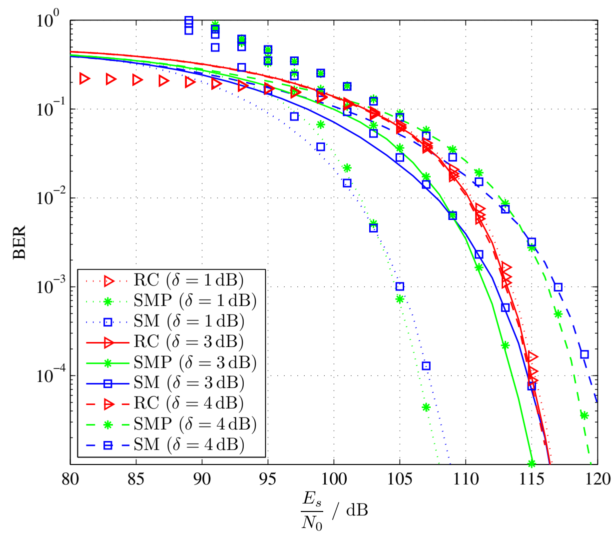

(b) $d_{\mathrm{TX}} = 0.6$ m

Fig. 7. Comparison of RC, SMP and SM for spectral efficiency of $R = 4$ bit/s/Hz in 4×4 setup scenario for varying power imbalances δ (lines show simulation results and markers analytical error bounds).

(5) and (11), whereas now $\tilde{I}_{n_t}$ is the mean optical power used for modulation by transmitter n_t.

Fig. 7 depicts the BER of RC, SMP and SM for a spectral efficiency of 4 bit/s/Hz in the 4×4 setup scenario with $d_{\mathrm{TX}} = 0.2$ m and $d_{\mathrm{TX}} = 0.6$ m for varying power imbalances. As shown, adding an imbalance to the transmission powers can enhance the performance of both SMP and SM, whereas it has no influence on RC. By imbalancing the power, the correlation of the single links is reduced making them more distinguishable at the receiver side. The receiver does not need any knowledge about the induced power imbalance because it implicitly gets this information by channel estimation which it performs anyway. Therefore to the receiver, the power imbalance appears to be due to the actual channel propagation. Consequently, imbalancing transmit powers does not increase the receiver's detection complexity. The performance of RC is not related to link differences but only to the absolute channel gains. Therefore, power imbalance has no effect on the performance of RC given the symmetrical arrangement of the channel gains denoted in (14). The results for the $d_{\mathrm{TX}} = 0.2$ m scenario shown in Fig. 7(a) indicate that a power imbalance of about $\delta = 1$ dB results in the best BER performance for SM, whereas for SMP $\delta = 3$ dB gives the lowest BER. More pronounced power imbalances lead to worse error ratios. While the correlation of the links may be reduced, the transmission power for some of the links is largely decreased in this case. This leads to a low SNR on these links and consequently, to a worse BER performance. Therefore, a compromise between channel correlation and appropriate signal detection is required. This is also the reason why SMP can operate with higher power imbalances compared to SM. SM has to operate with a larger signal constellation size to provide the same data rate, thus making it more susceptible to low SNRs. Consequently, SMP can profit to a larger extent by power imbalancing and achieves the same performance as RC. Note that the channel conditions without power imbalancing caused SMP to perform significantly worse than RC and SM in this scenario (see Fig. 3(a)). For $d_{\mathrm{TX}} = 0.6$ m, power imbalance has a negative effect on SMP and SM as their performance decreases with rising δ as shown in Fig. 7(b). Thus, no further benefits can be achieved and $\delta = 0$ dB gives the best performance for both SMP and SM.

C. Link blockage

In this section, we consider the $d_{\mathrm{TX}} = 0.2$ m and 0.4 m setups with an induced link blockage between some transmitters and receivers. This can be achieved by installing opaque boundaries in the receiver device or by smaller FOVs of the optical receivers. We assume the channel coefficients as given in (14) and block the same links of the 4×4 setup as in the $d_{\mathrm{TX}} = 0.6$ m scenario: the links between TX_1 and RX_4; TX_2 and RX_3; TX_3 and RX_2; TX_4 and RX_1. This results in the following channel matrices for the two setups with induced link blockage:

$$\widehat{\mathbf{H}}_{d_{\mathrm{TX}}=0.2} \approx 10^{-4} \begin{pmatrix} 1.0708 & 0.9937 & 0.9937 & 0.0000 \\ 0.9937 & 1.0708 & 0.0000 & 0.9937 \\ 0.9937 & 0.0000 & 1.0708 & 0.9937 \\ 0.0000 & 0.9937 & 0.9937 & 1.0708 \end{pmatrix} \tag{20}$$

resulting in $\widehat{\Delta}^{E_{\mathrm{RX}}}_{d_{\mathrm{TX}}=0.2} \approx -2.29\,\mathrm{dB}$ and

$$\widehat{\mathbf{H}}_{d_{\mathrm{TX}}=0.4} \approx 10^{-4} \begin{pmatrix} 0.9226 & 0.7964 & 0.7964 & 0.0000 \\ 0.7964 & 0.9226 & 0.0000 & 0.7964 \\ 0.7964 & 0.0000 & 0.9226 & 0.7964 \\ 0.0000 & 0.7964 & 0.7964 & 0.9226 \end{pmatrix} \tag{21}$$

resulting in $\widehat{\Delta}^{E_{\mathrm{RX}}}_{d_{\mathrm{TX}}=0.4} \approx -3.99\,\mathrm{dB}$.

Fig. 8 depicts the BER of RC, SMP and SM for $R = 4$ bit/s/Hz in these two setups. Relative to the results without link blockage, RC performs about 2 dB worse. This is because the induced link blockage leads to a lower SNR at the receiver. However, the performance of SM and SMP is significantly enhanced. Although there is less energy received, both MIMO schemes profit from the reduced channel correlation. Especially SMP, which performs worst without link blockage, benefits from the reduced channel correlation and provides the lowest error ratio in this scenario. The $d_{\mathrm{TX}} = 0.2$ m setup with induced link blockage provides the best compromise between channel correlation and received energy. As shown, both SM and SMP perform about 2 dB better compared to the setup with $d_{\mathrm{TX}} = 0.4$ m and induced link blockage. Relative to the $d_{\mathrm{TX}} = 0.6$ m setup (see Fig. 3(a)), SM and SMP achieve an even larger performance gain of about 5 dB.

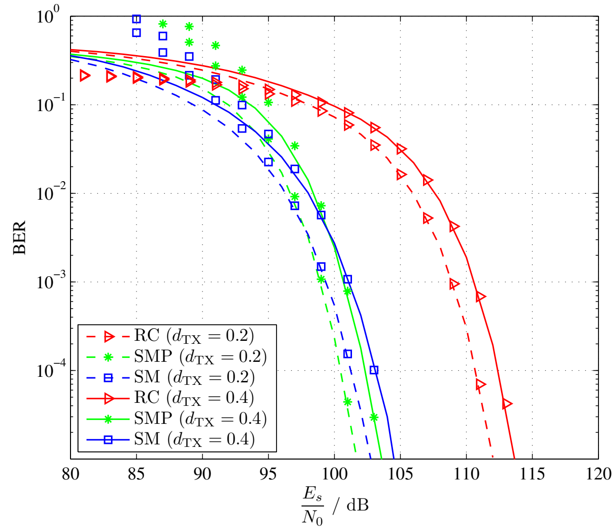

Fig. 8. Comparison of RC, SMP and SM for spectral efficiency of $R = 4$ bit/s/Hz in 4×4 setup scenario with $d_{\mathrm{TX}} = 0.2$ m and 0.4 m with induced link blockage (lines show simulation results and markers analytical error bounds).

V. Summary and Conclusion

In this paper, we have studied the performance of MIMO techniques applied to OWC in indoor environments. Several 4×4 setups with different spacings of the transmitters and different positions of the receiver array have been considered. We have shown that for OWC, MIMO schemes can provide gains even under static LOS conditions – channel conditions which commonly disallow the use of MIMO techniques in the RF domain. It has been shown that SMP improves the spectrum efficiency in IM/DD transmission systems. In order to achieve these improvements, sufficiently low channel correlations are required. Similarly, SM achieves improved spectral efficiencies especially at low SNRs and it is more robust to high channel correlation. SM enjoys additional implementation advantages as it only requires low complexity detection algorithms. This is because SM prevents ICI. RC is insensitive to different transmitter-receiver alignments, but suffers from the fact that it requires large signal constellation sizes to provide high data rates. It has been found that induced power imbalance between the transmitters is an effective technique to improve the BER performance. Under conditions which cause high channel correlation, power imbalance can enhance the performance of both SMP and SM remarkably. Consequently, if the transmission power is imbalanced, SMP and SM can even be used in scenarios which typically disallow the application of MIMO schemes. As shown, the best performance for the considered 4×4 indoor scenario can be achieved by blocking some of the 16 links between the transmitters and receivers. This induced blocking reduces the SNR at the receiver side. However, blocking 4 links, for example, improves the BER of both SMP and SM, since it outweighs the loss in SNR by reducing the channel correlation. These two MIMO techniques capitalise on both SNR and channel differences. Therefore, the induced link blockage represents the most suitable compromise between channel correlation and received energy for the considered scenarios. This work has also demonstrated that practical OWC systems could greatly benefit from adaptive MIMO techniques.

References

[1] Y. Tanaka, T. Komine, S. Haruyama, and M. Nakagawa, "Indoor visible communication utilizing plural white LEDs as lighting," in *Proc. 2001 IEEE International Symp. Personal, Indoor Mobile Radio Commun.*, vol. 2, pp. 81–85.

[2] T. Komine and M. Nakagawa, "Fundamental analysis for visible–light communication system using LED lights," *IEEE Trans. Consumer Electron.*, vol. 50, no. 1, pp. 100–107, Feb. 2004.

[3] K.-D. Langer, J. Grubor, O. Bouchet, M. El Tabach, J. Walewski, S. Randel, M. Franke, S. Nerreter, D. O'Brien, G. Faulkner, I. Neokosmidis, G. Ntogari, and M. Wolf, "Optical wireless communications for broadband access in home area networks," in *Proc. 2008 International Conf. Transparent Optical Netw.*, vol. 4, pp. 149–154.

[4] F. R. Gfeller and U. Bapst, "Wireless in-house data communication via diffuse infrared radiation," *Proc. IEEE*, vol. 67, no. 11, pp. 1474–1486, Nov. 1979.

[5] J. M. Kahn and J. R. Barry, "Wireless infrared communications," *Proc. IEEE*, vol. 85, no. 2, pp. 265–298, Feb. 1997.

[6] S. Hranilovic, *Wireless Optical Communication Systems*, 1st edition. Springer, 1996.

[7] D. O'Brien, H. L. Minh, L. Zeng, G. Faulkner, K. Lee, D. Jung, Y. Oh, and E. T. Won, "Indoor visible light communications: challenges and prospects," *Proc. SPIE, Free-Space Laser Commun. VIII*, vol. 7091, no. 1, p. 709106, 2008.

[8] R. Mesleh, H. Elgala, and H. Haas, "Optical spatial modulation," *J. Optical Commun. Netw.*, vol. 3, no. 3, pp. 234–244, Mar. 2011.

[9] E. Telatar, "Capacity of multi-antenna gaussian channels," *European Trans. Telecommun.*, vol. 10, no. 6, pp. 585–595, Nov. 1999.

[10] G. J. Foschini and M. J. Gans, "On limits of wireless communications in a fading environment when using multiple antennas," *Wireless Personal Commun.*, vol. 6, no. 3, pp. 311–335, Mar. 1998.

[11] S. G. Wilson, M. Brandt-Pearce, Q. Cao, and M. Baedke, "Optical repetition MIMO transmission with multipulse PPM," *IEEE J. Sel. Areas Commun.*, vol. 23, no. 9, pp. 1901–1910, Sep. 2005.

[12] S. Navidpour, M. Uysal, and M. Kavehrad, "BER performance of free-space optical transmission with spatial diversity," *IEEE Trans. Wireless Commun.*, vol. 6, no. 8, pp. 2813–2819, Aug. 2007.

[13] D. O'Brien, "Multi-input multi-output (MIMO) indoor optical wireless communications," in *Conf. Record 2009 Asilomar Conf. Signals, Syst., Comput.*, pp. 1636–1639.

[14] L. Zeng, D. O'Brien, H. Minh, G. Faulkner, K. Lee, D. Jung, Y. Oh, and E. T. Won, "High data rate multiple input multiple output (MIMO) optical wireless communications using white LED lighting," *IEEE J. Sel. Areas Commun.*, vol. 27, no. 9, pp. 1654–1662, Dec. 2009.

[15] T. Fath, M. Di Renzo, and H. Haas, "On the performance of space shift keying for optical wireless communications," in *Proc. 2010 IEEE Global Commun. Conf. - Workshop Optical Wireless Commun.*, pp. 990–994.

[16] O. Bouchet, G. Faulkner, L. Grobe, E. Gueutier, K.-D. Langer, S. Nerreter, D. O'Brien, R. Turnbull, J. Vucic, J. Walewski, and M. Wolf, "Deliverable D4.2b physical layer design and specification," *Seventh Framework Programme Information Commun. Technol.*, Feb. 2011, retrieved July 18, 2012 from http://www.ict-omega.eu.

[17] D. O'Brien, G. Faulkner, H. Le Minh, O. Bouchet, M. El Tabach, M. Wolf, J. Walewski, S. Randel, S. Nerreter, M. Franke, K.-D. Langer, J. Grubor, and T. Kamalakis, "Home access networks using optical wireless transmission," in *Proc. 2008 IEEE International Symp. Personal, Indoor Mobile Radio Commun.*, pp. 1–5.

[18] M. Safari and M. Uysal, "Do we really need OSTBCs for free-space optical communication with direct detection?" *IEEE Trans. Wireless Commun.*, vol. 7, no. 11, part 2, pp. 4445–4448, 2008.

[19] S. M. Alamouti, "A simple transmit diversity technique for wireless communications," *IEEE J. Sel. Areas Commun.*, vol. 16, no. 8, pp. 1451–1458, Oct. 1998.

[20] J. Armstrong, "OFDM for optical communications," *IEEE/OSA J. Lightw. Technol.*, vol. 27, no. 3, pp. 189–204, Feb. 2009.

[21] S. Dimitrov, S. Sinanovic, and H. Haas, "Signal shaping and modulation for optical wireless communication," *IEEE/OSA J. Lightw. Technol.*, vol. 30, no. 9, pp. 1319–1328, May 2012.

[22] D. Barros, S. Wilson, and J. Kahn, "Comparison of orthogonal frequency-division multiplexing and pulse-amplitude modulation in indoor optical wireless links," *IEEE Trans. Commun.*, vol. 60, no. 1, pp. 153–163, Jan. 2012.

[23] A. Goldsmith, *Wireless Communications*. Cambridge University Press, 2005.

[24] Y. A. Chau and S.-H. Yu, "Space modulation on wireless fading channels," in *Proc. 2001 IEEE Veh. Technol. Conf. – Fall*, vol. 3, pp. 1668–1671.

[25] R. Mesleh, H. Haas, S. Sinanović, C. W. Ahn, and S. Yun, "Spatial modulation," *IEEE Trans. Veh. Technol.*, vol. 57, no. 4, pp. 2228–2241, July 2008.

[26] R. Mesleh, M. Di Renzo, H. Haas, and P. M. Grant, "Trellis coded spatial modulation," *IEEE Trans. Wireless Commun.*, vol. 9, no. 7, pp. 2349–2361, July 2010.

[27] E. Basar, U. Aygolu, E. Panayirci, and V. H. Poor, "Space-time block coded spatial modulation," *IEEE Trans. Commun.*, vol. 59, no. 3, pp. 823–832, Mar. 2011.

[28] R. Mesleh, H. Haas, C. W. Ahn, and S. Yun, "Spatial modulation–a new low complexity spectral efficiency enhancing technique," in *Proc. 2006 IEEE International Conf. Commun. Netw. China*, pp. 1–5.

[29] R. Mesleh, "Spatial modulation: a spatial multiplexing technique for efficient wireless data transmission," Ph.D. dissertation, Jacobs University, Bremen, Germany, June 2007.

[30] A. Younis, M. Di Renzo, R. Mesleh, and H. Haas, "Sphere decoding for spatial modulation," in *Proc. 2011 IEEE International Conf. Commun.*, pp. 1–6.

Thilo Fath holds a Diploma in Information Technology from the University of Cooperative Education Mannheim, Germany (2004). During his course of studies he was student trainee at the Heidelberger Druckmaschinen AG, where he worked in several IT departments with focus on network and software technology. In 2008 he received the MSc degree in Electrical Engineering and Information Technology with focus on communication technology from the University of Karlsruhe, Germany. In August 2008, he joined EADS Innovation Works Germany, where he currently works on optical wireless communications. Since 2010, he has been with the Institute for Digital Communications (IDCOM) at the University of Edinburgh, UK, where he is working towards his Ph.D. degree in Electrical Engineering. His main research interests are in the area of digital signal processing with a particular focus on MIMO techniques and optical wireless communications.

Harald Haas (SM'98-AM'00-M'03) holds the Chair of Mobile Communications in the Institute for Digital Communications (IDCOM) at the University of Edinburgh and he currently is the CTO of a university spin-out company VLC Ltd. His main research interests are interference coordination in wireless networks, spatial modulation and optical wireless communications. Prof. Haas holds 23 patents. He has published more than 50 journal papers including a Science Article and more than 150 peer-reviewed conference papers. Nine of his papers are invited papers. Prof. Haas has co-authored a book entitled "Next Generation Mobile Access Technologies: Implementing TDD" with Cambridge University Press. Since 2007 Prof. Haas has been a Regular High Level Visiting Scientist supported by the Chinese "111 program" at Beijing University of Posts and Telecommunications (BUPT). He was an invited speaker at the TED Global conference 2011, and his work on optical wireless communications was listed among the "50 best inventions in 2011" in the Time Magazine. He received the EPSRC Established Career Fellowship in 2012.